Journal of Applied Mechanics and Technical Physics, Vol. 39, No. 3, 1998

CRITERION OF FORMATION OF A SHOCK WAVE REFLECTED FROM A CLOUD OF PARTICLES

S. P. Kiselev and V. P. Kiselev

UDC 662.612.32

The problem of the formation of a "collective" shock wave reflected from a cloud of particles, which was previously observed in experiment, is considered. A criterion of formation of a reflected shock wave is obtained based on the numerical and analytical solutions of the problem.

It was found in experimental studies [1] of the interaction of a shock wave (SW) with a cloud of Plexiglass and bronze particles that a "collective" shock wave reflected from the cloud is formed if the volume concentration of the particles is $m_2 \sim 10^{-2}$. A numerical solution of this problem gave the same results [2]. A criterion of formation of a "collective" SW is obtained in the present work based on numerical and approximate analytical solutions [2, 3].

We consider the formulation of the problem. There is a plane channel filled with air (Fig. 1). A cloud of spherical particles is located in the domain Ω. A SW is incident on the cloud from the left. The flow of gas and particles that results from the interaction of the SW with the cloud of particles is calculated by the numerical method described in [2]. Depending on the parameters of the gas and the particles, a reflected SW or a compression wave can arise ahead of the cloud. We seek a condition for the formation of a reflected SW.

The shock-wave intensity is characterized by the flow Mach number M_f in the coordinate system in which the shock wave is in the quiescent state. To distinguish between the SW and compression wave in the calculations, we assume that we have a shock wave for $M_f \geqslant 1.15$ and a compression wave for $M_f < 1.15$. In the case of $M_f \geqslant 1.15$, the entropy increment ΔS behind the SW satisfies the inequality [4]

$$\frac{\Delta S}{R} = \frac{2\gamma}{3(\gamma+1)^2}(M_f^2 - 1)^3 \geqslant 5.4 \cdot 10^{-3}.$$

Here R is the universal gas constant and γ is the Poisson's ratio of specific heats. For $M_f < 1.15$, the change in entropy can be ignored, the flow can be considered isentropic and the compression wave acoustic; M_f is defined as $M_f = (v_1 - D_f)/c_1$, where v_1 is the free-stream velocity, c_1 is the speed of sound, and D_f is the reflected wave velocity. It is seen from this formula that M_f is the Mach number of the reflected SW. For $M_f \geqslant 1.15$, according to [5], we obtain

$$p/p_1 \geqslant 1.38, \tag{1}$$

where p_1 and p are the pressures in front of and behind the reflected SW, respectively. Formula (1) is used as the condition of formation of the reflected SW, which is convenient for numerical calculations.

Let m_2^* be the volume concentration of particles for which $p/p_1 = 1.38$ and let a reflected shock wave be formed ahead of the cloud. The quantity m_2^* is a function of the parameters $m_2^* = m_2^*(\rho_{11}, \rho_{22}, v_1, c_1, h, l_r, \gamma)$, where ρ_{11} and ρ_{22} are the densities of the gas and the particles, h is the cloud length, and l_r is the relaxation length of the particles. We compose dimensionless complexes from these parameters (ρ_{11}/ρ_{22}, $M = v_1/c_1$, and h/l_r) and seek a solution as the product of the functions

$$m_2^* = \xi(\rho_{11}/\rho_{22})\,\varphi(h/l_r)\,\psi(M) \quad (\gamma = \text{const}).$$

Institute of Theoretical and Applied Mechanics, Siberian Division, Russian Academy of Sciences, Novosibirsk 630090. Translated from Prikladnaya Mekhanika i Tekhnicheskaya Fizika, Vol. 39, No. 3, pp. 44–51, May–June, 1998. Original article submitted May 30, 1996; revision submitted September 30, 1996.

 0021-8944/98/3903-0362 $20.00

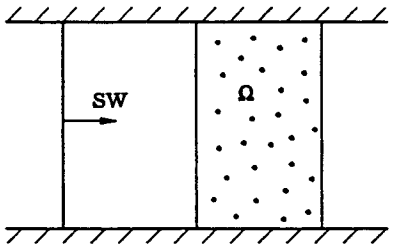

Fig. 1

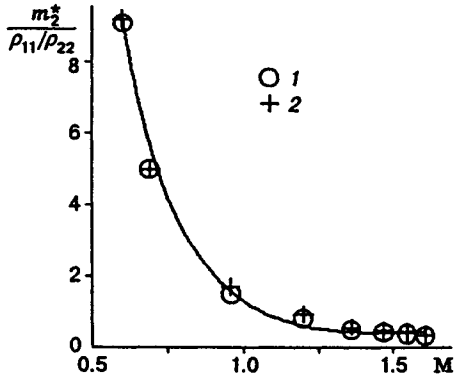

Fig. 2

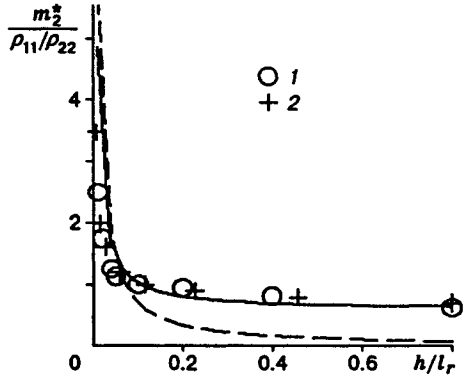

Fig. 3

The form of these functions obtained by approximation of numerical calculations is presented below.

The time of formation of the reflected SW is of the order of the time of gas deceleration [2]:

$$\tau_v = \frac{4}{3}\frac{d}{C_d|v_1 - v_2|}\frac{1}{m_2/m_1}.$$

Here C_d is the particle drag coefficient and m_1 and m_2 are the volume concentrations of the gas and the particles, related as $m_1 + m_2 = 1$. It is necessary that the gas and particle velocities did not have time to become equal during the time of formation of the reflected SW. Thus, the maximum pressure p behind the reflected wave is obtained for $\tau_v \sim \tau_{12}$. According to [6], the characteristic time of relaxation of the relative velocity of the gas and the particles is

$$\tau_{12} = \frac{4}{3}\frac{d}{C_d|v_1 - v_2|}\frac{1}{\rho_{11}/\rho_{22} + m_2/m_1}.$$

This condition is fulfilled if $\rho_{11}/\rho_{22} \sim m_2^*/m_1$; whence it follows that $m_2^* \sim \rho_{11}/\rho_{22}$. Therefore, the function ξ can be chosen in the form $\xi = \rho_{11}/\rho_{22}$. (We are dealing with the lower boundary of m_2 where the reflected SW is already arising.) The numerical calculations of this paper and the approximate analytical solution of (7) and (8) support this choice of the function ξ. Being treated in the coordinates $m_2^*/(\rho_{11}/\rho_{22})$, h/l_p, M, the results for bronze and Plexiglass fall on one curve (Figs. 2 and 3).

The functions $\psi(\mathrm{M})$ and $\varphi(h/l_r)$ are obtained by approximation of the results of numerical calculations. Figure 2 shows the dependence of $m_2^*/(\rho_{11}/\rho_{22})$ on M for $h/l_r = 0.4$. Here points 1 refer to the numerical results for Plexiglass particles, points 2 correspond to bronze particles, and the curve was obtained by the approximation formula

$$\varphi(0.4)\,\psi(\mathrm{M}) = \frac{9.26}{\mathrm{M}^2} - \frac{12.8}{\mathrm{M}} + 4.84. \tag{2}$$

The ratio $m_2^*/(\rho_{11}/\rho_{22})$ versus h/l_r for M = 1.3 is plotted in Fig. 3. Points 1 and 2 denote the same as

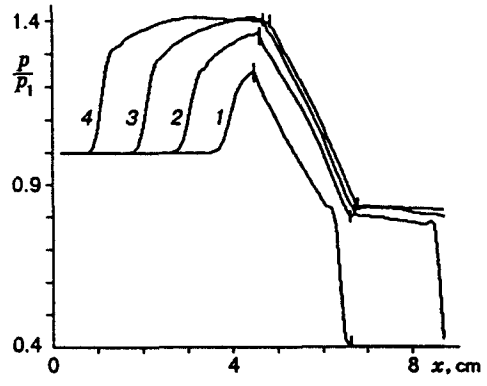

Fig. 4

in Fig. 2, and the curve corresponds to the approximation formula

$$\psi(1.3)\varphi(h/l_r) = \frac{4.27 \cdot 10^{-2}}{h/l_r} + 0.597. \tag{3}$$

Combining formulas (2) and (3), we find the desired dependence

$$m_2^* = \frac{\rho_{11}}{\rho_{22}}\left(\frac{0.09}{h/l_r} + 1.26\right)\left(\frac{9.26}{M^2} - \frac{12.8}{M} + 4.84\right). \tag{4}$$

We consider an example of formation of a reflected SW. Let a SW with a Mach number of $M_0 = 1.5$ be incident on a cloud of particles. The cloud consists of Plexiglass particles with $d = 10^{-2}$ cm, $\rho_{22} = 1.2$ g/cm^3, and $h = 2$ cm. The gas density behind the SW is $\rho_{11} = 2.34 \cdot 10^{-3}$ g/cm^3, the flow Mach number is $M = 0.6$, and $l_r = 14.4$ cm. The volume concentration of the particles calculated from (4) is $m_2^* = 3.25 \cdot 10^{-2}$.

Figure 4 shows calculated curves of p/p_1 versus x for times 50, 100, 150, and 200 μsec (curves 1–4, the vertical bars indicate the cloud boundaries). The calculations were performed for a gas pressure $p_1 = 2.44$ atm behind the incident shock wave and an initial volume concentration of particles $m_2^0 = 3.25 \cdot 10^{-2}$. It is seen from Fig. 4 that the compression wave formed in the forepart of the cloud increases with time, its front becomes steeper because of nonlinear effects, and this wave becomes a reflected SW. Hence it follows that formula (4) agrees with the numerical data.

Kiselev and Kiselev [3] constructed an approximate analytical solution that describes the gas flow in a rarefied cloud of particles ($m_2 \sim 10^{-3}$). The motion of particles was ignored, since, initially, $v_1 \gg v_2$. The effect of the cloud was considered as a small perturbation. The equations for the gas were expanded into a series in the small parameter m_2, and linear terms of the expansion were retained. The linearized equations were solved by the method of characteristics.

For the nondimensionalized perturbations of the gas velocity $v = v'/v_0$, density $\eta = \rho'/\rho_0$, and entropy $s = S'/c_V$ (the subscript 0 refers to the free-stream parameters and the prime denotes the perturbations), we obtain the following equations:

$$v = \frac{1}{2}\left(\int\limits_{C_+} \varphi\,dt + \int\limits_{C_-} \varphi\,dt\right), \quad s = \int\limits_{C_0} \psi\,dt, \quad \eta = \frac{1}{2}\frac{v_0}{a_0}\left(\int\limits_{C_+} \varphi\,dt - \int\limits_{C_-} \varphi\,dt\right),$$

$$\varphi = \varphi_1 + \varphi_2, \quad \psi = \psi_1 + \psi_2, \quad \varphi_1 = -\frac{a_0^2}{\gamma v_0}\frac{\partial s}{\partial x}, \quad \varphi_2 = -\frac{m_2^0}{\tau}\int\limits_{-\infty}^{x} (\delta(y) - \delta(y-h))dy,$$

$$\psi_1 = m_2^0\frac{\gamma(\gamma-1)M^2}{\tau}\int\limits_{-\infty}^{x} (\delta(y) - \delta(y-h))dy, \quad \psi_2 = -m_2^0\frac{1 - T_2^0/T_1^0}{\omega}\int\limits_{-\infty}^{x} (\delta(y) - \delta(y-h))\,dy.$$

Here a_0 is the speed of sound, $M = v_0/a_0$, T_1^0 and T_2^0 are the temperatures of the gas and the particles,

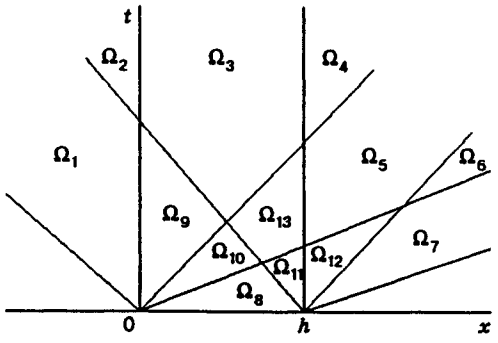

Fig. 5

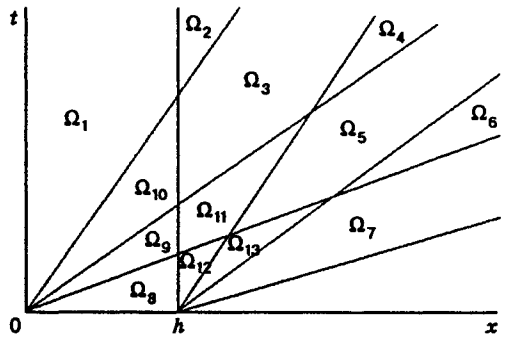

Fig. 6

$\tau = 4d/(3C_d v_0)$, $\omega = d^2\rho_{11}^0 c_V/(6\lambda \mathrm{Nu})$, c_V and λ are the thermal capacity and thermal conductivity of the gas, Nu is the Nusselt number, and $\delta(y)$ and $\delta(y-h)$ are the delta functions. The integration was performed along the characteristics

$$C_\pm\colon\ x = (v_0 \pm a_0)t + \xi_\pm, \qquad C_0\colon\ x = v_0 t + \xi_0.$$

The solution is split into 13 domains by the characteristics with constants $\xi_+ = \xi_- = \xi_0 = 0$, $\xi_+ = \xi_- = \xi_0 = h$ and the straight lines $x = 0$ and $x = h$, as is shown in Figs. 5 and 6 for $\mathrm{M} < 1$ and $\mathrm{M} > 1$, respectively.

The term proportional to $\partial s/\partial t$ is missing in formulas (3.6) and (3.7) of [3]. Allowance for this term yields

$$\int\limits_{C_+} \varphi_1 dt = \frac{a_0^2}{\gamma v_0(v_0 + a_0)}\left(-s + \int\limits_{C_+} \frac{\partial s}{\partial t}\,dt\right), \quad \int\limits_{C_-} \varphi_1 dt = \frac{a_0^2}{\gamma v_0(v_0 - a_0)}\left(-s + \int\limits_{C_-} \frac{\partial s}{\partial t}\,dt\right).$$

Ignoring the heat transfer, we write a corrected solution. For subsonic flow, we have

$$v' = -\frac{m_2^0}{2\tau}\left(v_0 t + \frac{\mathrm{M}x}{1-\mathrm{M}}\right)(1 + (\gamma-1)\mathrm{M}) \quad \text{in } \Omega_1,$$

$$v' = -\frac{m_2^0}{2\tau}\frac{\mathrm{M}h}{1-\mathrm{M}}(1 + (\gamma-1)\mathrm{M}) \quad \text{in } \Omega_2,$$

$$v' = -\frac{m_2^0 h\mathrm{M}}{2\tau(1-\mathrm{M})}\left(1 + (\gamma-1)\mathrm{M} - \frac{2\gamma\mathrm{M}}{1+\mathrm{M}}\frac{x}{h}\right) \quad \text{in } \Omega_3, \Omega_{13},$$

$$v' = -\frac{m_2^0}{2\tau}\frac{\mathrm{M}h}{1+\mathrm{M}}(1 - (\gamma-1)\mathrm{M}) \quad \text{in } \Omega_4, \Omega_5, \Omega_6,$$

$$v' = -\frac{m_2^0}{2\tau}\left(v_0 t - \frac{(x-h)\mathrm{M}}{1+\mathrm{M}}\right)(1 - (\gamma-1)\mathrm{M}) \quad \text{in } \Omega_7, \quad v' = -\frac{m_2^0}{\tau} v_0 t \quad \text{in } \Omega_8,$$

$$v' = -\frac{m_2^0}{2\tau}\left(v_0 t(1 + (\gamma-1)\mathrm{M}) + x\mathrm{M}\frac{1 - (\gamma-1)\mathrm{M}}{1+\mathrm{M}}\right) \quad \text{in } \Omega_9, \Omega_{10},$$

$$v' = -\frac{m_2^0}{2\tau}\left(v_0 t(1 - (\gamma-1)\mathrm{M}) + (x-h)\mathrm{M}\frac{1 + (\gamma-1)\mathrm{M}}{1-\mathrm{M}}\right) \quad \text{in } \Omega_{11},$$

$$v' = -\frac{m_2^0}{2\tau}\left(v_0 t + (x-h)\frac{\mathrm{M}}{1+\mathrm{M}}\right)(1 - (\gamma-1)\mathrm{M}) \quad \text{in } \Omega_{12},$$

$$\rho' = \frac{m_2^0 \mathrm{M}\rho_0}{2a_0\tau}\left(a_0 t + \frac{x}{1-\mathrm{M}}\right)(1 + (\gamma-1)\mathrm{M}) \text{ in } \Omega_1, \quad \rho' = \frac{m_2^0 \mathrm{M}\rho_0 h}{2a_0\tau}\frac{1 + (\gamma-1)\mathrm{M}}{1-\mathrm{M}} \text{ in } \Omega_2,$$

$$\rho' = \frac{m_2^0 \mathrm{M}\rho_0}{a_0\tau(1-\mathrm{M})}\left(-\frac{\gamma x}{1+\mathrm{M}} + \frac{h}{2}(1 + (\gamma-1)\mathrm{M})\right) \quad \text{in } \Omega_3,$$

$$\rho' = -\frac{m_2^0 \mathrm{M}\rho_0 h}{2a_0\tau}\,\frac{(\gamma-1)\mathrm{M}+2\gamma-1}{1+\mathrm{M}} \quad \text{in } \Omega_4, \tag{5}$$

$$\rho' = \frac{m_2^0 \mathrm{M}\rho_0}{a_0\tau}\left((\gamma-1)(x-v_0t) - \frac{h}{2}\,\frac{(\gamma-1)\mathrm{M}+2\gamma-1}{1+\mathrm{M}}\right) \quad \text{in } \Omega_5,$$

$$\rho' = -\frac{m_2^0 \mathrm{M}\rho_0 h}{2a_0\tau}\,\frac{1-(\gamma-1)\mathrm{M}}{1+\mathrm{M}} \text{ in } \Omega_6, \quad \rho' = \frac{m_2^0 \mathrm{M}\rho_0}{2a_0\tau}\left(\frac{x-h}{1+\mathrm{M}} - a_0t\right)(1-(\gamma-1)\mathrm{M}) \text{ in } \Omega_7,$$

$$\rho' = 0 \text{ in } \Omega_8, \quad \rho' = \frac{m_2^0 \mathrm{M}\rho_0}{2a_0\tau}\left(a_0t(1+(\gamma-1)\mathrm{M}) - x\,\frac{(\gamma-1)\mathrm{M}+2\gamma-1}{1+\mathrm{M}}\right) \text{ in } \Omega_9,$$

$$\rho' = \frac{m_2^0 \mathrm{M}\rho_0}{2a_0\tau}\left(a_0t - \frac{x}{1+\mathrm{M}}\right)(1-(\gamma-1)\mathrm{M}) \text{ in } \Omega_{10},$$

$$\rho' = \frac{m_2^0 \mathrm{M}\rho_0}{2a_0\tau}\left(\frac{h-x}{1-\mathrm{M}} - a_0t\right)(1+(\gamma-1)\mathrm{M}) \text{ in } \Omega_{11},$$

$$\rho' = \frac{m_2^0 \mathrm{M}\rho_0}{2a_0\tau}\left((x-h)\,\frac{(\gamma-1)\mathrm{M}+2\gamma-1}{1+\mathrm{M}} - a_0t(1+(\gamma-1)\mathrm{M})\right) \quad \text{in } \Omega_{12},$$

$$\rho' = \frac{m_2^0 \mathrm{M}\rho_0}{a_0\tau}\left(-(\gamma-1)v_0t - \left(1+\frac{\gamma\mathrm{M}^2}{1-\mathrm{M}^2}\right)x + \frac{h}{2}\,\frac{1+(\gamma-1)\mathrm{M}}{1-\mathrm{M}}\right) \quad \text{in } \Omega_{13},$$

$$S' = 0 \text{ in } \Omega_1, \Omega_2, \Omega_6, \Omega_7, \quad S' = m_2^0 c_V \gamma(\gamma-1)\mathrm{M}^2 x/(v_0\tau) \text{ in } \Omega_3, \Omega_9,$$

$$S' = m_2^0 c_V \gamma(\gamma-1)\mathrm{M}^2 t/\tau \quad \text{in } \Omega_8, \Omega_{10}, \Omega_{11}, \Omega_{13},$$

$$S' = m_2^0 c_V \gamma(\gamma-1)\mathrm{M}^2(v_0t - x + h)/(v_0\tau) \quad \text{in } \Omega_5, \Omega_{12},$$

$$S' = m_2^0 c_V \gamma(\gamma-1)\mathrm{M}^2 h/(v_0\tau) \quad \text{in } \Omega_4.$$

The qualitative curve of $v'(x)$ constructed in accordance with (5) for a fixed time t is shown in Fig. 7. A compression wave propagates toward the gas flow which slows down in this wave, while in the cloud, the gas is accelerated in the rarefaction wave. We note that the previously observed [3] difference between the numerical and analytical solutions in the domain Ω_4 has disappeared.

For supersonic flow, the solution is

$$v' = -\frac{m_2^0}{\tau}\,\frac{\gamma\mathrm{M}^2}{\mathrm{M}^2-1}\,x \text{ in } \Omega_1, \qquad v' = -\frac{m_2^0}{\tau}\,\frac{\gamma\mathrm{M}^2}{\mathrm{M}^2-1}\,h \text{ in } \Omega_2,$$

$$v' = -\frac{m_2^0}{2\tau}\left(\frac{2\gamma\mathrm{M}^2 h}{\mathrm{M}^2-1} + \left(v_0t - \frac{\mathrm{M}}{\mathrm{M}-1}x\right)(1+(\gamma-1)\mathrm{M})\right) \quad \text{in } \Omega_3, \Omega_{11},$$

$$v' = -\frac{m_2^0}{2\tau}\,\frac{\mathrm{M}h}{\mathrm{M}+1}(1-(\gamma-1)\mathrm{M}) \quad \text{in } \Omega_4, \Omega_5, \Omega_6,$$

$$v' = -\frac{m_2^0}{2\tau}\left(v_0t - (x-h)\,\frac{\mathrm{M}}{\mathrm{M}+1}\right)(1-(\gamma-1)\mathrm{M}) \text{ in } \Omega_7, \Omega_{13}, \qquad v' = -\frac{m_2^0}{\tau}v_0t \text{ in } \Omega_8,$$

$$v' = -\frac{m_2^0}{2\tau}\left(v_0t(1+(\gamma-1)\mathrm{M}) + x\,\frac{\mathrm{M}}{\mathrm{M}+1}(1-(\gamma-1)\mathrm{M})\right) \quad \text{in } \Omega_9, \Omega_{10},$$

$$v' = -\frac{m_2^0}{\tau}\left(v_0t - \frac{\gamma\mathrm{M}^2}{\mathrm{M}^2-1}(x-h)\right) \quad \text{in } \Omega_{12},$$

$$\rho' = \frac{m_2^0\gamma\mathrm{M}\rho_0}{a_0\tau(\mathrm{M}^2-1)}\,x \text{ in } \Omega_1, \quad \rho' = \frac{m_2^0\gamma\mathrm{M}\rho_0}{a_0\tau(\mathrm{M}^2-1)}\,h \text{ in } \Omega_2,$$

$$\rho' = \frac{m_2^0 \mathrm{M}\rho_0}{2a_0\tau}\left(\frac{2\gamma h}{\mathrm{M}^2-1} + a_0t(1+(\gamma-1)\mathrm{M}) - \frac{1+(\gamma-1)\mathrm{M}}{\mathrm{M}-1}x\right) \quad \text{in } \Omega_3,$$

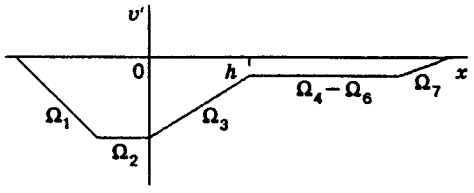

Fig. 7

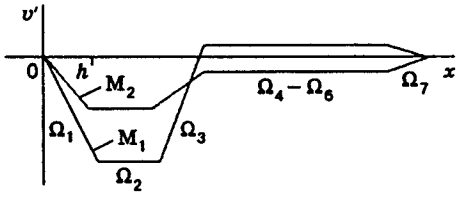

Fig. 8

$$\rho' = -\frac{m_2^0 \mathrm{M}\rho_0 h}{2a_0\tau}\,\frac{(\gamma-1)\mathrm{M}^2+1+\gamma(\mathrm{M}-2)}{\mathrm{M}^2-1} \quad \text{in } \Omega_4,$$

$$\rho' = \frac{m_2^0 \mathrm{M}\rho_0}{2a_0\tau}\left(2(\gamma-1)(x-v_0t) - h\,\frac{(\gamma-1)\mathrm{M}^2+1+\gamma(\mathrm{M}-2)}{\mathrm{M}^2-1}\right) \quad \text{in } \Omega_5, \tag{6}$$

$$\rho' = \frac{m_2^0 \mathrm{M}\rho_0 h}{2a_0\tau}\,\frac{(\gamma-1)\mathrm{M}-1}{\mathrm{M}+1} \text{ in } \Omega_6, \quad \rho' = \frac{m_2^0 \mathrm{M}\rho_0}{2a_0\tau}\left(\frac{h-x}{\mathrm{M}+1}+a_0t\right)((\gamma-1)\mathrm{M}-1) \text{ in } \Omega_7,$$

$$\rho' = 0 \text{ in } \Omega_8, \quad \rho' = \frac{m_2^0 \mathrm{M}\rho_0}{2a_0\tau}\left(\frac{x}{\mathrm{M}+1}-a_0t\right)((\gamma-1)\mathrm{M}-1) \text{ in } \Omega_9,$$

$$\rho' = \frac{m_2^0 \mathrm{M}\rho_0}{2a_0\tau}\left(a_0t(1+(\gamma-1)\mathrm{M}) - x\,\frac{(\gamma-1)\mathrm{M}^2+1+\gamma(\mathrm{M}-2)}{\mathrm{M}^2-1}\right) \quad \text{in } \Omega_{10},$$

$$\rho' = \frac{m_2^0 \mathrm{M}\rho_0}{2a_0\tau}\left(a_0t(1-(\gamma-1)\mathrm{M}) + \frac{x}{\mathrm{M}+1}\left((\gamma-1)\mathrm{M}-1-\frac{2\gamma}{\mathrm{M}-1}\right)+\frac{2\gamma h}{\mathrm{M}^2-1}\right) \text{ in } \Omega_{11},$$

$$\rho' = \frac{m_2^0 \gamma \mathrm{M}\rho_0}{a_0\tau}\,\frac{x-h}{\mathrm{M}^2-1} \quad \text{in } \Omega_{12},$$

$$\rho' = \frac{m_2^0 \mathrm{M}\rho_0}{2a_0\tau}\left((x-h)\,\frac{(\gamma-1)\mathrm{M}^2+1+\gamma(\mathrm{M}-2)}{\mathrm{M}^2-1} - a_0t(1+(\gamma-1)\mathrm{M})\right) \text{ in } \Omega_{13},$$

$$S' = 0 \text{ in } \Omega_6, \Omega_7, \quad S' = m_2^0 c_V \gamma(\gamma-1)\mathrm{M}^2 x/(v_0\tau) \text{ in } \Omega_1, \Omega_{10},$$

$$S' = m_2^0 c_V \gamma(\gamma-1)\mathrm{M}^2 t/\tau \quad \text{in } \Omega_8, \Omega_9,$$

$$S' = m_2^0 c_V \gamma(\gamma-1)\mathrm{M}^2(v_0t-x+h)/(v_0\tau) \quad \text{in } \Omega_5, \Omega_{11}, \Omega_{12}, \Omega_{13},$$

$$S' = m_2^0 c_V \gamma(\gamma-1)\mathrm{M}^2 h/(v_0\tau) \quad \text{in } \Omega_2, \Omega_3, \Omega_4.$$

A comparison of systems (6) and (3.12) from [3] shows that the solution of (3.12) is true in Ω_1. Hence, all inferences about the dependence $\mathrm{M}(x)$ drawn on the basis of this equation are also true. System (5) and (6) is also valid for a cloud of particles of finite dimensions which suddenly enters a uniform gas flow. We note that formulas (5) and (6) are inapplicable in the vicinity of the point $\mathrm{M} = 1$.

Figure 8 shows the function $v'(x)$ for the flow Mach numbers M_1 and M_2, where $\mathrm{M}_1 < \mathrm{M}_* < \mathrm{M}_2$, $\mathrm{M}_* = 1/(\gamma-1)$. It is evident that the gas is decelerated in the cloud and accelerated in the rarefaction wave behind the cloud. For $\mathrm{M} > \mathrm{M}_*$, the gas acquires a velocity higher than the gas velocity ahead of the cloud. This is related to the high pressure in the cloud and the adiabatic gas expansion behind the cloud. This effect is confirmed by results of numerical calculations (see Fig. 9, where $v = v_0 + v'$ and the vertical bars indicate the cloud boundaries). At the entrance to the cloud, the gas has the following parameters: $\mathrm{M} = 4$, $\rho_{11} = 10^{-3}$ g/cm^3 and $v_0 = 1.36 \cdot 10^5$ cm/sec. The parameters of the cloud of particles are as follows: $m_2^0 = 10^{-3}$, $\rho_{22} = 1.2$ g/cm^3, $h = 1$ cm, and $d = 100$ μm.

We evaluate the condition of formation of the reflected SW using the approximate solution (5) and (6). The compression wave that arises ahead of the cloud of particles is formed in the domain Ω_2. Therefore, we use the solution from Ω_2 to calculate this wave.

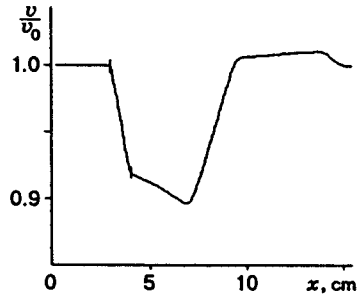

Fig. 9

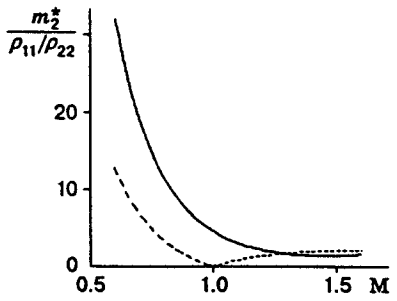

Fig. 10

According to (1), we assume that the reflected shock wave is formed if $p'/p_1 \approx \rho'/\rho_1 + S'/c_V \approx 0.4$, where p', ρ', and S' are the perturbations of the gas pressure, density, and entropy due to the interaction with the cloud of particles. Substituting ρ' and S' from (5), we obtain the condition of formation of the reflected SW for $M < 1$:

$$m_2^* = \frac{0.8}{\gamma}\frac{\rho_{11}}{\rho_{22}}\frac{1}{h/l_p}\frac{1-M}{M^2(1+(\gamma-1)M)}. \tag{7}$$

For supersonic flow, a similar substitution from (6) yields the analytical solution

$$m_2^* = \frac{0.4}{\gamma^2}\frac{\rho_{11}}{\rho_{22}}\frac{1}{h/l_r}\frac{M^2-1}{M^2+(1-1/\gamma)M^2(M^2-1)}. \tag{8}$$

The dashed curve in Fig. 3 shows the ratio $m_2^*/(\rho_{11}/\rho_{22})$ versus h/l_r obtained using formula (8). The analytical and numerical results are in good agreement for $h/l_r < 0.1$. For larger values of h/l_r, the analytical and numerical solutions are different, and this leads to the difference in the values of m_2^*.

Figure 10 shows a comparison of the numerical (the solid curve) and analytical (the dashed curve) solutions for the curve of $m_2^*/(\rho_{11}/\rho_{22})$ versus M for $h/l_r = 0.04$. These solutions are in good agreement in the supersonic-flow region. In the vicinity of $M = 1$, the analytical solution is inoperative, and the difference for $M < 1$ occurs because m_2^* lies in a region in which the approximate solution yields a significant error.

REFERENCES

1. V. M. Boiko, A. V. Fedorov, V. M. Fomin, et al., "Ignition of small particles behind shock waves", in: *Progress in Astronautics and Aeronautics*, Vol. 87: *Shock Waves, Explosions, and Detonations* (1987), pp. 71–87.
2. V. P. Kiselev, S. P. Kiselev, and V. M. Fomin, "Interaction of a shock wave with a cloud of particles of finite dimensions," *Prikl. Mekh. Tekh. Fiz.*, **35**, No. 2, 26–37 (1994).
3. S. P. Kiselev and V. P. Kiselev, "Some features of the flow of gas that occurs as a result of the interaction between a shock wave and a cloud of particles," *Prikl. Mekh. Tekh. Fiz.*, **36**, No. 2, 8–18 (1995).
4. L. G. Loitsyanskii, *Mechanics of Liquids and Gases*, Pergamon Press, Oxford-New York (1966).
5. B. L. Rozhdestvenskii and N. N. Yanenko, *Systems of Quasi-Linear Equations and Their Applications to Gas Dynamics* [in Russian], Nauka, Moscow (1978).
6. S. P. Kiselev, G. A. Ruev, A. P. Trunev, et al., *Shock-Wave Processes in Two-Species and Two-Phase Media* [in Russian], Nauka, Novosibirsk (1992).